Adsorption of elemental S on Si(100)2×1: Surface restoration

Aris Papageorgopoulos and Adero Corner
Department of Physics and Center for High Performance Polymers and Ceramics, Clark Atlanta University, Atlanta, Georgia 30314

M. Kamaratos and C. A. Papageorgopoulos
Department of Physics, University of Ioannina, P.O. Box 1186, GR-451 1 0 Ioannina, Greece
(Received 26 January 1996)

Adsorption of elemental S at room temperature causes the transition of the reconstructed Si(100)2×1 surface to its original bulk-terminated Si(100)1×1. The S adsorbate forms initially a (2×1) structure at 0.5 ML on the Si(100)2×1 surface, a (1×1) at 1 ML on the Si(100)1×1, and above 1 ML sulfur is imbedded into the Si substrate. The sticking coefficient of S is constant and equal to unity for the first 2 ML. Deposition of S at room temperature up to 1 ML increases the work function by 0.3±0.05 eV. The S adsorbate is strongly bound to the Si substrate in a molecular Si-S form. The Si-S bond energy is greater than that of Si-Si, which may be the driving force of the Si(100)2×1→Si(100)1×1 transition. [S0163-1829(97)01507-5]

I. INTRODUCTION

The passivation of semiconductor surfaces is an area of intrinsic scientific interest and of great technological importance. Silicon and other semiconductors, such as GaAs and InP, are well known for their potentially wide use in high-speed electronics and long-wavelength optical circuits (optoelectronics).[1,2] They have also demonstrated great value, mainly in space technology, as solar cells (photovoltaics).[3] Their efficiency, however, is reduced by electron,[4] x-ray,[5] and γ (Ref. 6) radiation damage. Nonradiative recombination of charge carriers[1] is another such cause. To prevent damage in the surfaces involved without reducing their efficiency the above semiconductors are passivated. This is done by depositing protective films (dielectric window layers), such as chalcogenides: sulfur, gallium sulfide, and indium sulfide.[7–10] Most of the studies concerning surface passivation of semiconductors were carried out with the use of chemical vapor deposition techniques under atmospheric pressure. The analysis of the deposited layers with the former techniques has been obtained *ex situ* after the completion of films a few hundred nm thick.

The *in situ* analysis of the initial stages of the interface formation in ultrahigh vacuum (UHV) is necessary for the understanding and subsequent improvement of the deposition process. The interface region between the adsorbate and the substrate is that which primarily controls the growth of the films. The understanding of the film growth, therefore, requires deposition methods that allow control of the building process of the structure at the atomic level.[11] A beginning with elemental S deposition on Si(100)2×1 in UHV would be appropriate. The knowledge of the behavior of S alone on Si and other semiconductors is very important because (a) of the interest that has arisen with respect to the possibility of pretreating the surfaces of the semiconductors with S to protect and stabilize these surfaces against degradation resulting in improved subsequent processing,[12,13] and (b) it will help to obtain a better understanding of the binding structure and electronic properties of the growth of chalcogenide protective films such as GaS and InS.

Besides the importance in applications, there is a recent rising scientific interest in the structural and electronic properties of chalcogen elements (S,Se) on Si(100)2×1 surfaces. Theoretical calculations suggest that adsorbates change the structure of the Si(100)2×1 surfaces.[14,15] To our knowledge, this does not agree with the up-to-date relevant experimental results. More specifically, the Si(100) surface is easily reconstructed with a small amount of heating. The surface has a structure different from that of the bulk, and the reconstruction of the clean surface occurs in order to reduce the number of broken dangling bonds.[14] In other words, the reconstruction of the surface minimizes the high energy of broken covalent bonds, which would exist on an ideal bulk-terminated plane.[15] The clean Si(100) surface shows a strong (2×1) reconstruction in the low-energy electron diffraction (LEED) pattern, observed for the first time by Schlier and Farnsworth in 1959.[16] Several models for the (2×1) reconstruction have been proposed.[17] It has been recently accepted by most researchers that dimers are the main building blocks of the reconstructed surface of Si(100). The question, however, of whether the dimers are symmetric or buckled remains unclear, as reported by Chadi.[18] Today, new evidence of asymmetric (buckled) dimers is supported by most of the experimental[19–23] and theoretical[14,15] investigators who have worked on this problem. Kruger and Pollman[14] calculated that buckled dimers are energetically favored over symmetric ones by 0.14 eV per dimer.[14] The restoration of reconstructed semiconductor surfaces to their original bulk-terminated surface has been achieved, lately, by different adsorbates. Specifically, ideal (1×1) terminations of (111) surfaces were reported for As on Ge(111) (Ref. 24) and Si(111) (Refs. 25 and 26) and for Cl on Ge(111).[27] Adsorption of S on clean Ge(100)2×1 changed the (2×1) structure to (1×1). The system S/Ge(100)1×1 was regarded as an ideally terminated surface.[28] Weser *et al.*[28] have experimentally investigated the behavior of S on Si(100). They have

not observed an ordered S adlayer. Moriarty, Koenders, and Hughes[30] reported, recently, that room-temperature adsorption of sulfur resulted in the formation of an overlayer with the underlying Si(100) retaining the (2×1) reconstruction. They also mentioned that annealing of the S/Si(100)2×1 surface to 325 °C leads to the desorption of the sulfur overlayer and the appearance of coexisting $c(4\times4)$ and (2×1) surface reconstruction. In contrast to this paper, theoretical studies performed by Kaxiras,[15] and later by Kruger and Pollman,[14] suggested that adsorption of group VI elements (S or Se) on Si(100)2×1 can lead to the restoration of the ideal bulk-terminated geometry on the semiconductor surfaces. From the above discussion it is apparently clear that additional effort on the study of S and Se on Si(100)2×1 is necessary.

Most of the sulfur adsorption studies up to now have taken place with the exposure of the substrates to H_2S gas. To remove the H_2 from the surface the substrates were heated to temperatures equal to or greater than 200 °C. Hydrogen, however, cannot be removed selectively. These mixed systems do not show any well-defined long-range order.[28] For a detailed understanding of the adsorption kinetics of S on Si surfaces at room and lower temperatures, it is important to deposit elemental sulfur.

In this work we evaporate elemental sulfur on Si(100)2×1 surfaces. We study the sample using LEED, Auger Electron Spectroscopy (AES), thermal-desorption spectroscopy (TDS), and work function (WF) measurements. The data suggest that the presence of sulfur on the surface causes a phase transition of the substrate. Preliminary results have been reported elsewhere.

II. EXPERIMENT

The experiments were performed in an ultrahigh vacuum chamber ($p<10^{-10}$ Torr), equipped with a cylindrical mirror analyzer (CMA) for AES measurements, a quadrupole mass spectrometer (QMS) for TDS measurements, a LEED system, and a Kelvin probe for WF measurements.

Elemental sulfur was evaporated by thermal dissociation of MoS_2 single crystal flakes mounted on a tungsten filament. During dissociation of MoS_2 the Mo remained on the tungsten filament, while S was evaporated. The Si(100) substrate was cleaned by Ar^+ bombardment at $E=1$ keV for 40 min with an ion current of 10 μA. After bombardment the sample was heated to 1000 °C by passing current through a 0.05-mm Ta strip, uniformly pressed between the sample and a Ta foil case. The temperature of the sample was measured by a Cr-Al thermocouple. The Si specimen was considered sufficiently clean when the Auger peak height ratios C(272 eV)/Si(92 eV) and O(512 eV)/Si(92 eV) were below 1%. The estimation of the S coverages on Si(100) surfaces were based on a correlation of LEED, AES, and TDS measurements, and the comparison with the measurements of S on the Ni(100) surface, which took place in the same system under the same deposition conditions.[31] The surface atomic density of 1 ML of S on Si(100) is considered equal to that of the outermost layer of Si, $N_{Si}=6.8\times10^{14}$ atoms cm^{-2}.

III. RESULTS

A. Auger and work-function measurements

Figure 1 shows the Auger peak-to-peak heights (AppH) of the S(151 eV) and the work function ($\Delta\Phi$) change as a function of the number of doses of S deposited on clean Si(100)2×1 surfaces at room temperature. These measurements are shown in correlation with the observed LEED patterns, which will be discussed later in the next section. As seen in this figure, the Auger peak-to-peak height of S(151 eV) initially increases linearly with an increasing number of S doses. Near the ninth dose, the curve forms a break (slope change of the S Auger peak height versus S dose curve). Also above the 9th dose the S Auger peak height is increasing linearly up to the 18th dose of our measurements where it forms a second break. Above the 18th dose the S(151 eV) peak height starts to level off. This Auger peak height versus S doses curve is characteristic of a layer-by-layer growth. During the S deposition on the clean Si(100)2×1 surface at room temperature, the work function initially increases linearly with increasing S coverage. Above the fourth S dose the work-function curve deviates from linearity and its slope becomes smaller. Near the ninth dose, the work function reaches its maximum value, and subsequently starts to decrease as the number of sulfur doses increases. Above the thirteenth dose the decrease of the work function is very small, despite that the Auger peak height of S(151 eV) continues to increase. The maximum observed value of the WF increase was about 0.3 eV. The above WF measurements were repeated three times, and the maximum WF value varied by ±0.05 eV. Figure 2 shows the energy shift of the integrated Auger Si(92 eV) peak during S deposition on clean Si(100)2×1. The inset shows the Si(92 eV) energy shift versus S doses. According to the inset, this shift increases linearly with increasing S doses to its final value of 1.5 eV at the completion of the second layer of S. During heating and as the S is removed from the surface the shift decreases and the energy of the Si peak goes back to that of the clean Si surface. This is an Auger chemical shift, which may be attributed to a strong S-Si interaction. Most likely, the S adatoms form a compound with the Si substrate. The fact that the shift increases linearly may indicate that the nature of binding is the same up to the completion of the second layer, in agreement with the following TDS measurements.

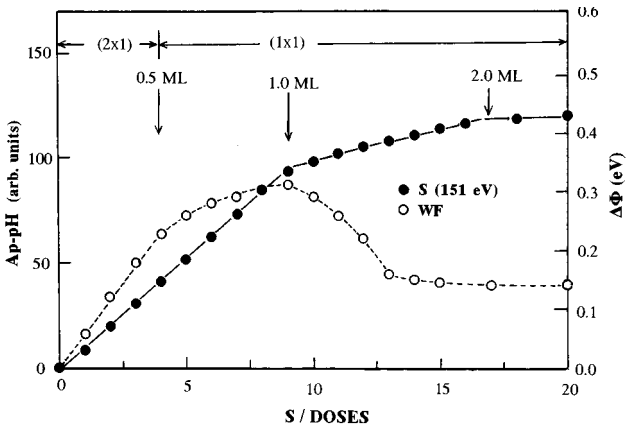

FIG. 1. Auger peak-to-peak heights (AppH) of the S(151 eV) and the work function ($\Delta\Phi$) change as a function of the number of doses of S deposited on clean Si(100)2×1 surfaces at room temperature.

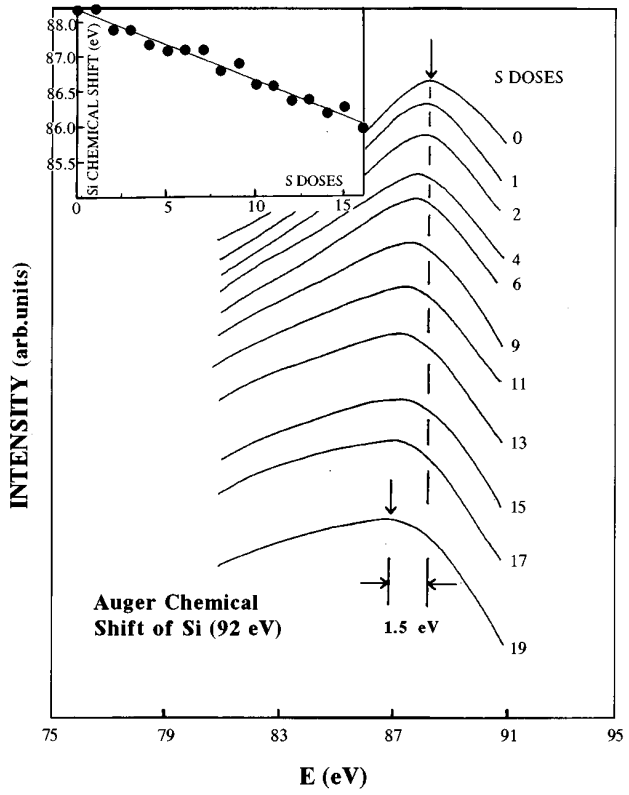

FIG. 2. Energy shift of the integrated Auger Si(92 eV) peak during S deposition on clean Si(100)2×1. The inset shows the Si chemical shift vs S doses.

B. TDS measurements

Thermal-desorption spectra from S-covered Si(100) surfaces have shown hardly observable peaks of S_2 (amu 64). Sulfur was mainly desorbed as a SiS compound. Figure 3 shows a series of SiS (amu 60) of thermal-desorption spectra for different amounts of S deposited on Si(100) surfaces. The heating rate of desorption was constant, β=30 K/s, for all

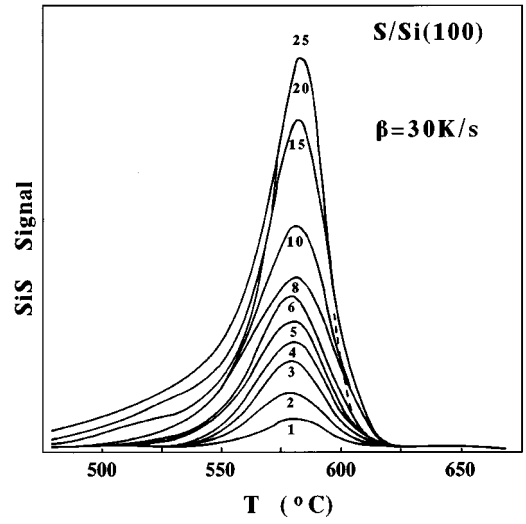

FIG. 3. Thermal-desorption spectra of SiS from S-covered Si(100) surfaces.

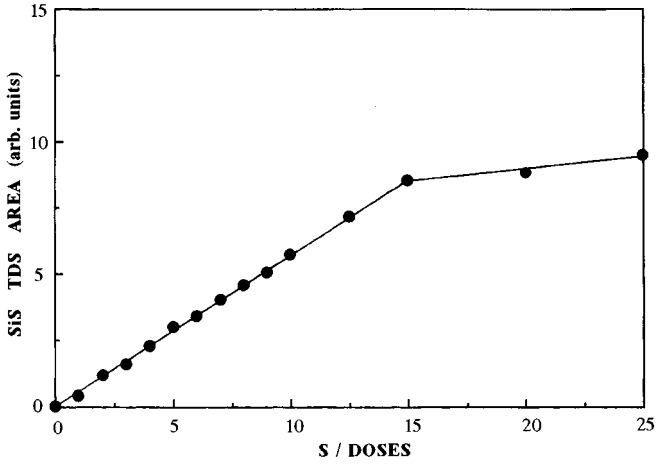

FIG. 4. Areas under the thermal desorption peaks of SiS (Fig. 3) vs S doses on Si(100) surfaces.

spectra. There is only a single peak with its maximum value near 585 °C, the very small peaks of S_2, not shown here, appear at the same temperature and probably are due to a partial dissociation of the SiS molecule. This finding does not agree with Moriarty, Koenders, and Hughes,[30] who reported that the annealing of the S-covered Si(100)2×1 surface to 325 °C leads to the desorption of the sulfur overlayer. The latter disagreement will be also discussed in correlation with other findings in the discussion. The fact that the TD peaks of SiS remain relatively sharp at the same temperature with increasing S coverage indicates that the nature of Si-S binding remains the same up to the completion of the S coverage corresponding to the completion of 2 ML, in agreement with the chemical shift measurements.

Figure 4 shows the areas under the TD peaks of SiS (Fig. 3) versus the S doses on Si(100) surfaces. Note that the S doses in the TDS were 15% greater than those in the previous (AES and WF) measurements, and the completion of 2 ML of S in Fig. 4 occurs at the 15th dose. It is obvious, from this figure, that the TDS areas increase linearly with increasing number of S doses, with a break (slope change of the SiS TDS areas versus S doses curve) occurring near the 15th dose of S; this is where we believe that the completion of 2 ML of sulfur takes place. It is known that the slope of the areas under the TDS versus doses of a deposited adsorbate on a substrate is proportional to the sticking coefficient of the adsorbate. This, in correlation with Fig. 4, implies that the sticking coefficient of S on Si(100) surfaces remains constant up to 2 ML and subsequently becomes substantially smaller.

C. LEED measurements

The LEED observations show that the clean Si(100)2×1 surface gives a good intense (2×1) LEED pattern. Above the fourth dose of S deposition on this surface, the half-order spots become diffused and the pattern changes to (1×1) with its maximum intensity near the ninth dose. Further S deposition increases the background, however, the (1×1) structure remains. It appears that above the 4th dose of S the Si(100)2×1 reconstructed surface begins to change to Si(100)1×1. We believe that S adsorption on Si(100)2×1

forms also a (2×1) structure, initially. The (2×1) pattern, near the 4th dose, should correspond to 0.5 ML of S coverage. Above the 4th dose, both the Si substrate and the S adsorbate change gradually to a (1×1) structure. The completion of the (1×1), near the 9th dose, corresponds to 1.0 ML of S, and coincides with the first break of the Auger curve and the maximum increase of the work-function value (Fig. 1). Above the 9th S dose, the (1×1) is retained.

The same UHV system has been used previously with the same S source, and about the same flux of S on Ni(100).[31] The LEED observations showed the formation of a $c(2\times2)$ pattern close to the 12th dose of S on Ni(100). The density of the S overlayer, which produces the $c(2\times2)$ on Ni(100), is 8×10^{14} atoms cm^{-2} at 12 doses. At 9 doses this density should be about 6×10^{14} atoms cm^{-2}. This is very close to 6.8×10^{14} atoms cm^{-2}, which is the density of 1 ML of S on Si(100). Therefore, at the completion of the (1×1) structure on Si(100), the coverage of S at 9 doses is indeed about 1 ML. It has been proposed that the initial sticking coefficient of S on clean Ni(100) is close to unity.[32] This implies that the initial sticking coefficient of S on Si(100)2×1 is also one. The linearity of the Auger curve up to 1 ML (Fig. 1) indicates that the sticking coefficient of S on Si(100) surface remains one, at least up to 1 ML. The slope of the Auger curve is also constant for the second monolayer, between the first and the second break, which occurs in about the same time of completion as that of the first monolayer. This may further imply that the sticking coefficient of S is nearly constant during the adsorption of the second S layer, between the 9th and 18th doses. Moreover, the TDS measurements (Fig. 4) indicate clearly that the sticking coefficient remains constant and, therefore, equal to unity up to the completion of 2 ML of S coverage.

Despite that the Auger curve remains linear and the sticking coefficient remains constant up to 9th S dose, the work-function curve deviates from linearity at the 4th dose. This may be attributed to different sites of S atoms on Si before and after the 4th dose. Both the chemical shift (Fig. 2) and the TDS (Fig. 4) measurements indicate that the nature of binding of S atoms on Si remains the same up to 2 ML of S, which may imply that the charge transfer (polarization) for each S adatom remains also the same. Therefore, any change to the surface dipole moment should be attributed to the dipole length change. Consequently, the sulfur atoms residing on the dimers of the Si(100)2×1 surface may have greater dipole moment (dipole length) than on sites between Si atoms of the Si(1×1) surface. In the latter case, the distance between the neighboring Si atoms of the top layer is greater than that between those of the dimers of the reconstructed surface. Therefore, the S adatoms should be deeper in their sites between the Si atoms of the (1×1) surface structure, with a smaller dipole length, therefore, smaller dipole moment and consequently a smaller work function than that for S atoms on the dimers. This will be explained in more detail in the Discussion. The fact that, above 1.0 ML (9th dose), the work-function value decreases, while the sticking coefficient and the nature of binding of S on Si remain constant, may indicate that above 1.0 ML the sulfur is submerged into the Si bulk near the surface. Since the WF lowering almost stops before the S coverage completion of 2 ML means that only part of the second layer is initially diffused into the bulk of Si at room temperature.

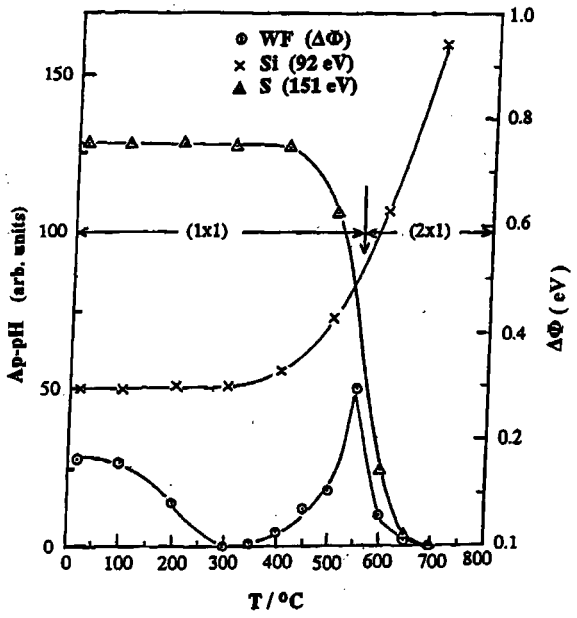

FIG. 5. Variation of the Auger peak-to-peak height (AppH) of S(151 eV) and the work-function change (ΔΦ) during the heating of the S-covered Si(100)2×1 surfaces.

D. Heating of S-covered Si(100)2×1 surfaces

Figure 5 shows the variation of the Auger peak-to-peak height of S(151 eV) and the work-function change (ΔΦ), in correlation with the LEED patterns, during the heating of the S-covered Si(100)2×1 substrate. The heating was implied in 50 °C increments for 2 min each. We should emphasize that the work function decreases in the early stages of the heating treatment and reaches its minimum value at 300 °C while the Auger peak height remains nearly unchanged up to 400 °C, i.e., at which the S is not yet removed from the surface. Most likely, heating provides the activation energy for diffusion of more S atoms into the bulk of the Si substrate, causing a further work-function decrease. Above 400 °C, the work function increases while the Auger peak of S decreases drastically, indicating a drastic desorption of S from the surface. At about 550 °C, the second S layer is removed completely and the work function increases to its maximum value of 1 ML. Above 550 °C the WF decreases again and as the S coverage approaches 0.5 ML, the surface changes back to the reconstructed (2×1). Near 650 °C the S is completely desorbed from the Si substrate.

IV. DISCUSSION

As we have mentioned previously, the current experimental LEED observations show very clearly that deposition of elemental sulfur on clean Si(100)2×1 surfaces, at room temperature, changes the Si(100)2×1 reconstructed surface to Si(100)1×1. We believe that the S adatoms initially reside on the dimers forming a (2×1) at 0.5 ML and a (1×1) above

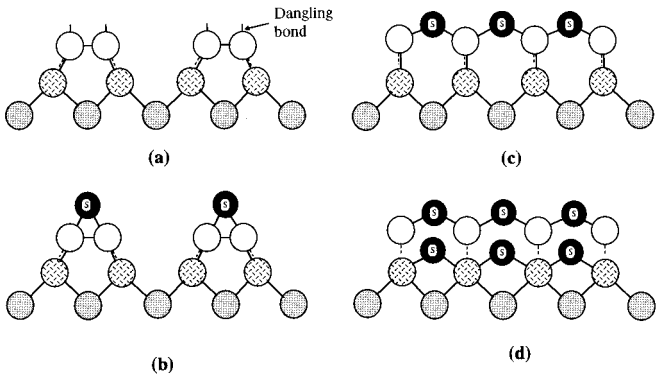

FIG. 6. Side-view schematics of (a) the top three layers of a clean reconstructed Si(100)2×1 surface with the dangling bonds, (b) the S-(2×1) (hemisulfide) structure on the Si(100)2×1 surface, (c) the S-(1×1) (monosulfide) structure on a Si(100)1×1 surface, and (d) the diffused second S layer into the bulk of Si(100)1×1.

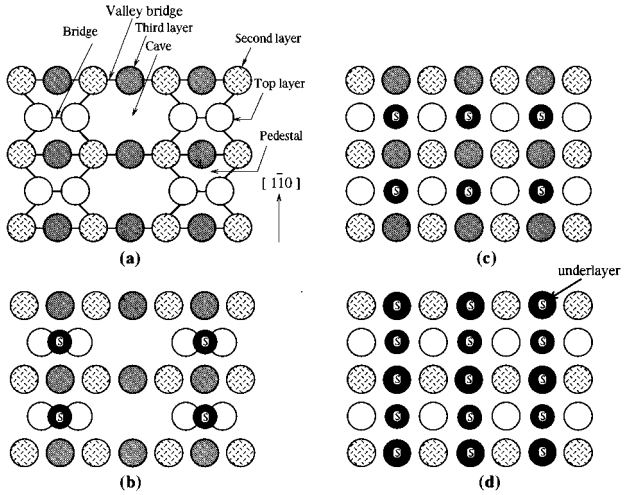

FIG. 7. Top-view schematics of (a) the top three layers of the clean reconstructed Si(100)2×1 surface, (b) the S-(2×1) structure on the Si(100)2×1 surface, (c) the S-(1×1) structure on Si(100)1×1 surface, and (d) the diffused second S layer into the bulk of Si(100)1×1.

this coverage. In Fig. 6 we propose a surface structural model of sulfur on Si(100) surfaces. Figure 6(a) shows a schematic side view of the top three layers of the clean reconstructed Si(100)2×1 surface with the dangling bonds. The deposited S atoms originally reside on bridge sites. Each S atom is specifically bound through the dangling bonds on the two Si atoms of the dimer [Fig. 6(b)], which is consistent with the fact that S is divalent. The maximum coverage of this state is 0.5 ML at which all the dimer sites are filled, and the S adatoms form a (2×1) structure retaining the reconstruction of the Si substrate. This (2×1) structure of the S overlayer on the Si(100)2×1 surface has been named the hemisulfide state. As the S deposition on the Si substrate continues above 0.5 ML, the S atoms that reside on available bridge sites between dimers cause the bonds between the Si atoms of the dimers to break, thus providing bonding for the S adatoms. As a result of this process, the Si atoms are gradually displaced, causing the restoration of the reconstructed Si(100)2×1 to a Si(100)1×1 surface. The sulfur adatoms remain on the bridge sites, and are bound to neighboring Si atoms as shown in Fig. 6(c). Thus, above 0.5 ML, S gradually forms a S(1×1) structure, causing the change of the Si substrate to an ideal bulk-terminated plane. This S(1×1) structure on Si(100)1×1 has been named the monosulfide state with a maximum coverage of 1 ML. Above 1 ML, S continues to be adsorbed with the same sticking coefficient up to the coverage of 2 ML. Most of the second monolayer of S is initially diffused into the bulk of Si and later the diffusion decreases and S remains on the surface. The heating of 300 °C provides activation energy for further diffusion with a simultaneous decrease of the WF. Figure 6(d) shows a possible binding of the embedded S atoms, which we call disulfide state. Figure 7 shows a top view of (a) a clean Si(100)2×1 surface, (b) the hemisulfide on Si(100)2×1, (c) the monosulfide on Si(100)1×1, and (d) the disulfide on Si(100)1×1.

The break of the bond between the Si atoms of the dimers and the subsequent rearrangement to a (1×1) structure is consistent with a strong Si-S interaction. This strong interaction is suggested by the chemical shift of the Auger Si(92 eV) peak during S deposition (Fig. 2) and the TDS measurements (Fig. 3). The latter measurements show that the S is desorbed as a SiS molecule, indicating clearly that the Si-S bond energy is greater than that of Si-Si, which may indeed be the dominant cause of the substrate restoration to Si(100)1×1. The greater S-Si bond energy than that of a Si-Si substrate has been reported some time ago.[33] The heating results (Fig. 5) indicate that, as soon as part of the S is desorbed from the surface and the coverage is $\leqslant$0.5 ML the reconstructed (2×1) comes back again. Our model of S adsorption on the Si substrate is in agreement with Kaxiras,[15] and later with Kruger and Pollman's[16] theoretical calculations. According to their results adsorption of S or Se causes the surface restoration of the reconstructed Si(100)2×1 substrate to its original bulk-terminated surface. Kaxiras, in his report, considered different structures consisting of embedding and mixing of the group-VI adatoms with Si substrate atoms. He emphasizes, however, that the restored surfaces are stable against all of the considered alternative structures. This is in agreement with our measurements, which indicate an imbedding of the second S layer into the Si bulk.

Next, we will try to justify the WF variations in correlation with the corresponding adsorption sites of S on the Si substrate. As is explained in Sec. III, the surface dipole moment changes are mainly due to those of the dipole length, which are dictated by site changes of the S on the Si substrate. However, the WF changes are proportional to the dipole moment [Eq. (1)].

From the initial slope of the WF curve (Fig. 1) the initial dipole moment of S may be calculated by the Hemholtz equation:

$$p_0=(1/2\pi)(\Delta\Phi/\Delta N)_{N\to 0}$$
$$=1/2\pi 300\times 10^{-18}(\Delta\Phi/\Delta N)_{N\to 0}\ \text{Debye}, \qquad (1)$$

where the sulfur atomic density $N=\Theta_S$ 6.8×10^{14} atoms cm^{-2}, and Θ_S is the coverage of S in monolayers. The

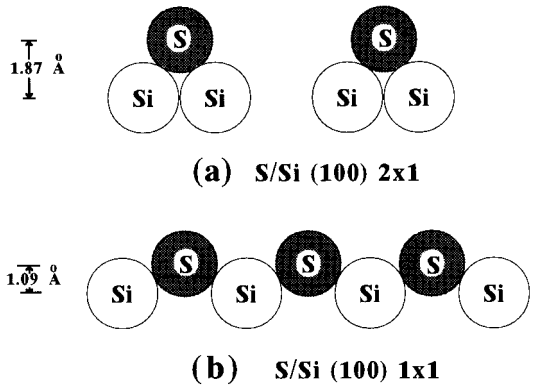

FIG. 8. Location of the S atoms (a) on the Si(100)2×1 surface, (b) on the Si(100)1×1 surface.

initial dipole moment of S was found to be $p_0=0.4$ Db (Debye). If it is considered that in the hemisulfide state the S atoms reside on the dimers as in Figs. 6(a) and 8(a), and that $p_0=qd$ or $q=p_0/d$, where q is the charge of each S adatom and $d=1.87$ A, it is found that $q=0.04e$ (where e is the charge of an electron). This indicates that the charge of the S overlayer is very small to consider the bonds of S on the Si substrate as ionic. Most likely, the S-Si bond is covalent, in agreement with the chemical shift (Fig. 2) and the TDS measurements (Fig. 3). After the restoration, the distance between the S overlayer and the topmost layer of the Si substrate decreases and becomes $d=1.09$ A [Fig. 8(b)]. Considering this dipole length and the finding that $q=0.04e$, it is found that $p_0=qd=0.2$ Db. Therefore, the value of p_0 is smaller in the monosulfide state than in the hemisulfide. This is consistent with the decrease in slope and deviation from linearity of the WF curve above 0.5 ML of S (4th dose) on Si(100) (Fig. 1), when the reconstructed (2×1) Si surface starts to change to its (1×1).

During the binding of S to the dimers of the Si substrate, we cannot preclude a decrease of the Si substrate WF due to a transition of the asymmetric dimers to their symmetric arrangement. It has already been mentioned in the Introduction: the existing view is that the dimers of the Si(100) are buckled. This asymmetric deformation increases the dipole moment of the dimers, and the WF is greater than that of the substrate with unbuckled (symmetric) dimers.[18,34] The existence of the asymmetric dimers is supported experimentally by ion scattering[19,20] and LEED experiments.[21] Recent STM (Refs. 22 and 23) measurements and theoretical calculations[14,15] make the view of asymmetric dimers even stronger. From our measurements it is not clear that the dimers remain asymmetric in the hemisulfide state or that during S deposition the asymmetric dimers change to symmetric. In the latter case, the increase of the work function during S deposition in the hemisulfide state would be compensated to some degree by the WF lowering during the transition of the asymmetric dimers to their symmetric state. The increase of the WF in the hemisulfide state, however, was very close to 0.25 eV measured (in the same UHV system) for 0.5 ML of S on the Ni(100) (Ref. 31) surface, which may indicate that the increase in WF up to 0.5 ML was due to the adsorption of S alone and not to any structural change of the dimers.

Besides the theoretical support[14,15] on the restoration of the semiconductor surfaces to their original bulk-terminated geometry achieved by S and Se adsorbates, there are also several experimental results mentioned in the Introduction. These results, however, refer to As on Ge(111) (Ref. 24) and on Si(111),[25,26] and to Cl on Ge(111).[27] Weser *et al.*[28] reported that S on Ge(100)2×1 changed the (2×1) structure to (1×1) and that the S/Ge(100)1×1 system was regarded as an ideal terminated surface. The same authors, however, have not observed any S overlayer on the Si(100)2×1 surface.[29] Recently, Moriarty, Koenders, and Hughes[30] reported that room-temperature adsorption of S resulted in the formation of an overlayer on Si(100)2×1, retaining the (2×1) reconstruction. They also report that annealing of S covered Si(100)2×1 at 325 °C leads to the desorption of the sulfur overlayer. As was already mentioned, the complete removal of S takes place by heating the substrate to 650 °C. The same authors, in continuing their investigation, discovered coexisting $c(4\times4)$ and (2×1) surface reconstructions after the desorption of S at 325 °C. Our finding that S is desorbed as a SiS molecule shows that heating causes depletion of Si from the surface. Annealing at relatively low temperatures would cause a partial removal of Si from the surface, which could change the reconstruction from (2×1) to a $c(4\times4)$. Although our structural models are consistent with the experimental results, we cannot rule out completely the possibility that, from the beginning of deposition, S forms two-dimensional islands of (1×1). Above a certain coverage, the islands coalesce, leading to a uniform (1×1) structure at 1 ML. More work is needed to be done.

V. CONCLUSION

The adsorption of elemental S at room temperature causes the change of the reconstructed Si(00)2×1 substrate to its original bulk-terminated Si(100)1×1 surface. The S adsorbate forms initially a (2×1) structure at 0.5 ML on the Si(100)2×1 substrate and subsequently a (1×1) on Si(100)1×1. Above 1 ML, sulfur is imbedded into the Si bulk near the surface. The sticking coefficient of S on the Si(100)2×1 surface is constant and equal to unity for the first 2 ML. Deposition of S at RT up to 1 ML increases the work function of the surface by about 0.3 ± 0.05 eV. Above 1 ML, as the sulfur is diffused into the Si bulk, the work function decreases. Surface dipole moment estimations based on the work-function measurements suggest that the Si-S bond is covalent. The deposition of S causes a chemical shift of the Si(92 eV) peak of 1.5 eV, indicating a strong S-Si interaction, while the TDS measurements show that S is mainly desorbed in the form of a SiS compound. This result supports the argument that the Si-S bond energy is greater than that of Si-Si, which may be the driving force of the Si(100)2×1→Si(100)1×1 transition.

ACKNOWLEDGMENTS

The authors wish to acknowledge the support of NASA Grant No. NCC3-286 and the NASA High Performance Polymers and Ceramics Center at Clark Atlanta University Grant No. NAGW-2939.

[1] A. N. MacInnes, M. B. Power, and A. R. Barron Appl. Phys. Lett. **62**, 711 (1993).
[2] R. R. Chang and D. L. Life, Appl. Phys. Lett. **53**, 134 (1988).
[3] R. K. Jain and G. A. Laundis (unpublished).
[4] M. Yamaguchi *et al.*, Appl. Phys. Lett. **44**, 432 (1984).
[5] A. Yamamoto, M. Yamaguchi, and C. Vemura, Appl. Phys. Lett. **44**, 611 (1984).
[6] I. Weinberg, C. K. Swartz, and R. E. Harf (unpublished).
[7] R. Leonelli, C. S. Sundaraman, and J. F. Currie, Appl. Phys. Lett. **57**, 2678 (1990).
[8] S. Shikoda, H. Okada, and H. Hayashi, J. Appl. Phys. **69**, 2717 (1991).
[9] A. N. MacInnes, M. B. Power, and A. P. Barron, Chem. Mater. **4**, 11 (1992).
[10] M. B. Power, A. N. MacInnes, A. F. Hepp, and A. R. Barron, in *Chemical Perspectives of Microelectronic Materials III*, edited by C. R. Abernathy *et al.*, MRS Soc. Symp. Proc. No. 282 (Materials Research Society, Pittsburgh, 1993), p. 659.
[11] A. Madhukar, Thin Solid Films **231**, 8 (1993).
[12] K. P. Pande and D. Gutierrez, Appl. Phys. Lett. **46**, 416 (1985).
[13] J. Chare, A. Choujaia, C. Santinelli, R. Blanchef, and P. Victorovitch, J. Appl. Phys. **61**, 257 (1987).
[14] Peter Kruger and Johannes Pollman, Phys. Rev. B **47**, 1898 (1993).
[15] Efthimios Kaxiras, Phys. Rev. B **43**, 6824 (1991).
[16] R. E. Schlier and H. E. Farnsworth, J. Chem. Phys. **30**, 917 (1959).
[17] *The Chemical Physics Of Solid Surfaces and Heterogenous catalysis*, edited by D. A. King and D. P. Woodruff (Elsevier, Amsterdam, 1988), Vol. 5, p. 37.
[18] D. J. Chadi, Phys. Rev. Lett. **43**, 43 (1979).
[19] R. M. Tromp, R. G. Smeenk, and F. W. Saris, Phys. Rev. Lett. **46**, 9392 (1981).
[20] M. Aono, Y. Hou, C. Oshima, and Y. Ishizawa, Phys. Rev. Lett. **49**, 567 (1982).
[21] B. W. Holland, C. B. Duke, and A. Paton, Surf. Sci. **140**, L 269 (1984).
[22] R. J. Hamers, R. M. Tromp, and J. E. Demuth, Phys. Rev. B **34**, 5343 (1986).
[23] R. A. Wolkow, Phys. Rev. Lett. **68**, 2636 (1992).
[24] R. D. Bringans, R. I. G. Uhrberg, R. Z. Bechrach, and J. E. Northrup, Phys. Rev. Lett. **55**, 533 (1985).
[25] R. D. Bringans, R. I. G. Uhrberg, and R. Z. Bechrach, Phys. Rev. B **34**, 2373 (1986).
[26] R. R. G. Uhrberg, R. D. Brigans, M. A. Olmstead, R. Z. Brachrach, and J. E. Northup, Phys. Rev. B **35**, 3945 (1987).
[27] R. D. Schnell, F. J. Himpsel, A. Bogen, D. Rieger, and W. Steinmann, Phys. Rev. B **32**, 8052 (1985).
[28] T. Weser, A. Bogen, B. Konrad, R. D. Schnell, C. A. Schug, W. Moritz, and W. Steinmann, Surf. Sci. **201**, 245 (1988).
[29] T. Weser, A. Bogen, B. Konrad, R. D. Schnell, C. A. Schug, and W. Steinmann, in *Proceedings of the 18th International Conference on the Physics of Semiconductors*, edited by O. Engstrom (World Scientific, Singapore, 1987), p. 97.
[30] P. Moriarty, L. Koenders, and G. Hughes, Phys. Rev. B **47**, 15 950 (1993).
[31] C. A. Papageorgopoulos and M. Kamaratos, Surf. Sci. **338**, 77 (1995).
[32] M. Blaszczyszyn, R. Blaszczyszyn, Z. Medewski, A. J. Melmed, and J. Madey, Surf. Sci. **131**, 433 (1983).
[33] M. Copel, M. C. Reuter, E. Kaxiras, and R. M. Tromp, Phys. Rev. Lett. **63**, 632 (1989).
[34] Woodruff and T. A. Delchar, *Modern Techniques of Surface Science* (Cambridge University Press, Cambridge, 1986).